Results in Physics 2 (2012) 182–184

Contents lists available at SciVerse ScienceDirect

Results in Physics

journal homepage: www.journals.elsevier.com/results-in-physics

Group velocity of the probe light in semiconductor–metal molecules

Zhi-Hong Xiao [a], HuiFang Zhang [b], HongZhen Lin [a,*]

[a] International Laboratory for Adaptive Bio-Nanotechology (i-LAB), Suzhou Institute of Nano-Tech and Nano-Bionica, CAS, Suzhou 215123, China
[b] Department of Physics, College of Science, Shanghai University, Shanghai 200444, China

ARTICLE INFO

Article history:
Received 7 August 2012
Accepted 25 September 2012
Available online 17 October 2012

Keywords:
Semiconductor-metal molecules
Coherent exciton–plasmon interaction
Group velocity

ABSTRACT

The group velocity of light is investigated in a hybrid nanostructure comprised of semiconductor quantum dot (SQD) and metal nanoparticle (MNP). In the presence of MNP, the hybrid absorption of the system can be eliminated and forms a broad transparency window even though related dipole transition is not forbidden. Owing to the presence of MNP, there is the formation of the steep dispersion at the transparency regime, thus, the controllable group velocity of light can be implemented. The group velocity of light is changed from subluminal to superluminal via adjusting the inter-particle distance between SQD and MNP.

Nanomaterials incorporating semiconductor quantum dot (SQD), metal nanoparticle (MNP), dye molecular, and metal surface have recently received great attention. For instance, the hybrid structure composed of semiconductor quantum dots (SQDs) and metal nanoparticles (MNPs) is focused due to its unique physical properties [1–9]. SQDs have many advantages, such as bright photo-luminescence, tunable color, and high photostability. Putting a SQD in the vicinity of a proper MNP, the SQD and the MNP are coupled by Coulomb interaction and the coupling strength depends on the geometry of the hybrid structure. In such hybrid structure, many new optical effects are investigated, such as exciton/plasmonic induced transparency [5,8], photonic induced diffraction grating [10], etc.

In this letter, we studied the group velocity of light in a SQD-MNP hybrid structure based on exciton/plasmonic induced transparency. When a proper coupling field is applied, the hybrid absorption of the system dramatically decreases until it vanishes in the presence of the MNP, and there is the steep dispersion at a transparency regime. Thus, the controllable group velocity of the probe light can be implemented. Further analysis shows that the light propagation can be changed from subluminal to superluminal by coherent exciton–plasmon interaction.

Fig. 1a describes a hybrid nanostructure composed of a spherical semiconductor quantum dot (SQD) with radius b and a spherical metal nanoparticle (MNP) of radius a. ε_b is the background dielectric constant. ε_s and ε_m are the dielectric constants of SQD and MNP, respectively. Δ_p and Δ_c denote the detuning given by $\Delta_p = \omega_{12} - \omega_p$ and $\Delta_c = \omega_{23} - \omega_c$, respectively. The SQD and MNP are separated by a distance R. Fig. 1b shows the energy scheme of the system. The plasmonic excitations of the MNP are a continuous spectrum; the excitations of the SQD are excitons with discrete energy levels. The interband transition $|2\rangle \leftrightarrow |3\rangle$ is excited by a strong coupling field with frequency ω_c and the Rabi frequency is given by $\Omega_c = \mu_{23}E_c/\hbar$, and a weak probe field with frequency ω_p drives the interband transition $|1\rangle \leftrightarrow |2\rangle$, and the Rabi frequency $\Omega_c = \mu_{12}E_c/\hbar$, where μ_{12} and μ_{23} are the transition dipole moments of the SQD.

The induced polarization of the probe light will be $P = \epsilon_b \chi E_p$, and $R \ll \lambda$, where λ is the wavelength of the probe field. Moreover, we use the dipole approximation, assuming $a, b < R$, where [10].

$$\mathrm{Im}(x^{(1)}) = \frac{-(1+K')}{[\Delta_p - E + \eta K''] \cdot \left(\frac{E-\Delta_p}{F+\gamma_{21}}\right) - (F+\gamma_{21})} \tag{1a}$$

$$\mathrm{Re}(x^{(1)}) = \frac{-(E-\Delta_p)(1+K')}{[\Delta_p - E + \eta K''] \cdot (E-\Delta_p) - (F+\gamma_{21})^2} \tag{1b}$$

where

$$E = \frac{|\Omega_c|^2(\Delta_p+\Delta_c)}{\gamma_{31}^2 + (\Delta_p+\Delta_c)^2}, F = \frac{\gamma_{31}^2 \cdot |\Omega_c|^2}{\gamma_{31}^2 + (\Delta_p+\Delta_c)^2}, K' = \frac{r \cdot a^3 \cdot S_\alpha}{\varepsilon_{\mathrm{effm}} \cdot R^3},$$
$$K'' = \frac{\mu_{12}^2}{4\pi\hbar\varepsilon_b}, \eta = \frac{r \cdot a^3 \cdot S_\alpha^2}{\varepsilon_{\mathrm{effm}} \cdot \varepsilon_{\mathrm{effs}} \cdot R^6}$$

$$\varepsilon_{\mathrm{effm}} = (2\varepsilon_b + \varepsilon_m)/3\varepsilon_b, \varepsilon_{\mathrm{effs}} = (2\varepsilon_b + \varepsilon_s)/3\varepsilon_b,$$
$$r = (\varepsilon_m - \varepsilon_b)/(2\varepsilon_b + \varepsilon_m).$$

The external applied fields are parallel to the major axis of the system ($S_a = 2$). Used parameters are $\mu_{12} = 0.67\mathrm{nm}, \gamma_{21} = 1\mathrm{ns}^{-1}$, $\gamma_{31} = 3\mathrm{ns}^{-1}, \epsilon_b = 1, \epsilon_s = 6, N = 3 \times 10^{21}\mathrm{m}^{-3}$.

* Corresponding author.
E-mail address: hzlin2010@sinano.ac.cn (H. Lin).

2211-3797 © 2012 Elsevier B.V. Open access under CC BY-NC-ND license.
http://dx.doi.org/10.1016/j.rinp.2012.09.009

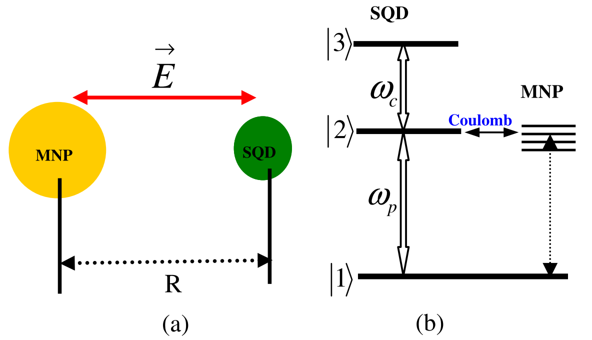

Figure 1. (a) Schematics of nanocrystal complex composed of spherical MNP and quantum dot; (b) Energy structure of the system, the horizontal arrow depicts the Coulomb interaction.

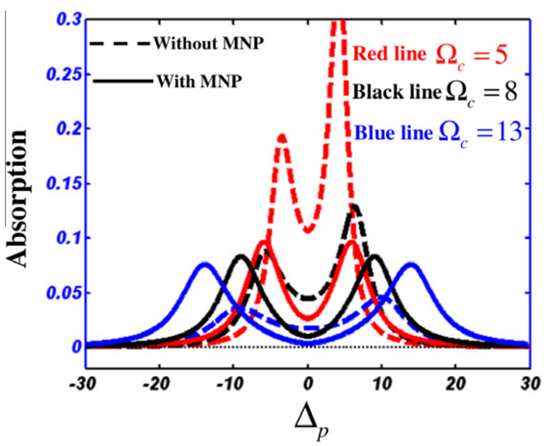

Figure 2. Absorption of the probe light versus probe detuning Δ_p with different Rabi frequency Ω_c with or without MNP. Used parameters: $\Delta_c = 0, \gamma_{21} = 1, \gamma_{31} = 1, \mu_{21} = 0.67$; and in the presence of MNP, $a = 6, S_a = 2, R = 33$ nm, $\varepsilon_b = 1, \varepsilon_s = 6$.

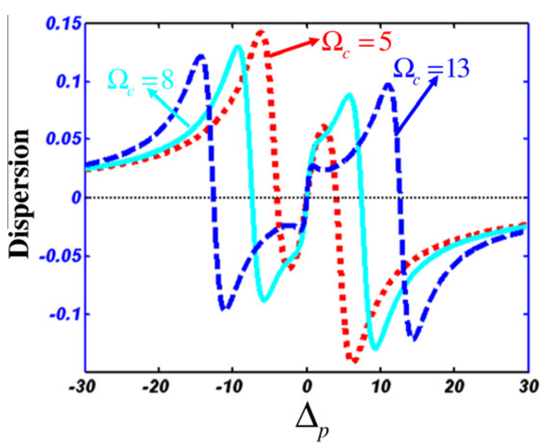

Figure 3. Dispersion of the probe light versus probe detuning Δ_p with different Rabi frequency Ω_c in the presence of MNP. Other parameters are the same as Fig. 2.

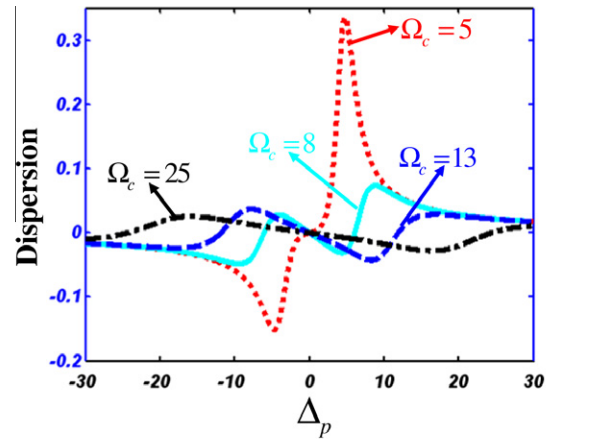

Figure 4. Dispersion of the probe light versus probe detuning Δ_p with different Rabi frequency Ω_c in the absence of MNP. Used other parameters are the same as Fig. 2.

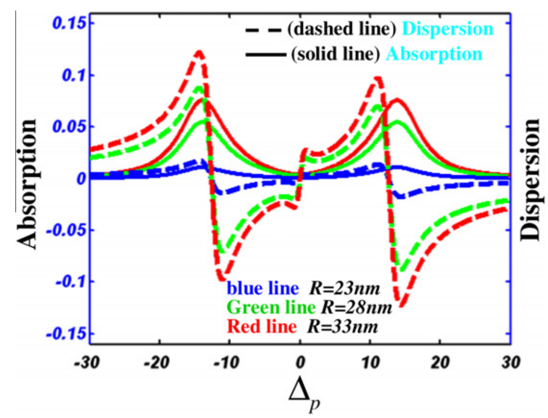

Figure 5. Absorption and dispersion of the probe light versus probe detuning Δ_p with different values of R in the presence of MNP. Used other parameters are the same as Fig. 2.

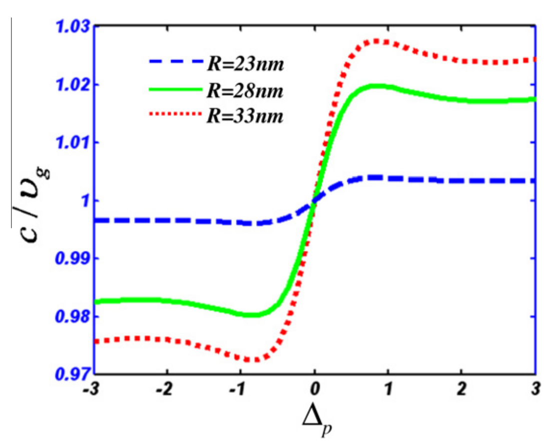

Figure 6. c/υ_g versus probe detuning with different values of R in the presence of MNP. Used other parameters are the same as Fig. 2.

In Figs. 2–4, the absorption and dispersion of the probe light are plotted with MNP and without MNP. In the presence of MNP, the dip on the absorption spectrum becomes deep until it forms a transparency window and the steep dispersion at the transparency region as increasing the intensity of the coupling field. The width of the transparency window becomes broad in comparison to conventional EIT investigated in the SQD systems. The absorption of the MNP can be controlled by adjusting the intensity of the coupling field when the MNP is at the vicinity of the SQD, and the strong absorption of the MNP is eliminated at near resonance [7]. The plasmonic induced transparency is formed due to the coherent interaction of the external coupling field with the SQD. The SQD

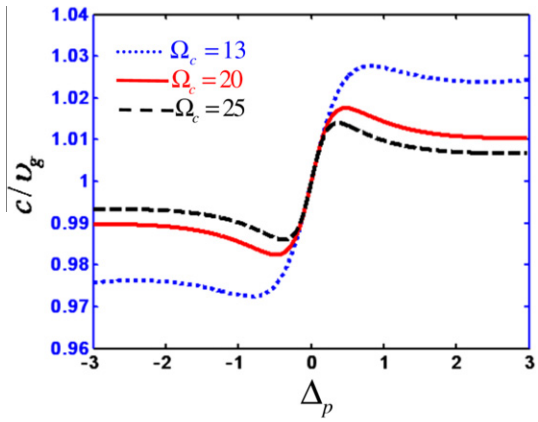

Fig. 7. c/υ_g versus probe detuning with different values of Ω_c in the presence of MNP. Used other parameters are the same as Fig. 2.

and the MNP are coupled due to the plasmonic resonance of the MNP, and transition $|1\rangle \leftrightarrow |3\rangle$ to generate the transparency that is not dipole forbidden. In the absence of the MNP, the steep dispersion cannot be obtained at the transparency regime.

The absorption and dispersion of the SQD-MNP hybrid system are depicted with different values of R in Fig. 5. The absorption and dispersion are influenced by the inter-particle distance R between the SQD and the MNP. The abrupt dispersion at transparency regime is achieved at large R. The interaction strength between the SQD and the MNP varies as R changes. So the R-dependent destructive or constructive interference causes the change in the absorption and dispersion.

It is well known that the group velocity of light is described by

$$\frac{c}{\upsilon_g} = 1 + 2\pi\mathrm{Re}(x) + 2\pi\omega\frac{d\mathrm{Re}(x)}{d\omega} \tag{2}$$

Then Fig. 6 illustrates the group velocity index as a function of detuning Δ_p for different values of R. It shows that the group velocity depends on the inter-particle distance R between the SQD and the MNP, i.e., can be controlled via the interaction strength between the SQD and the MNP. The value of group velocity index is close to 1 ($c \approx \upsilon_g$) at small R. The controllable group velocity of light is implemented from subluminal to superluminal at large R. It shows that the group velocity index is very sensitive to the inter-particle interaction distance R between the SQD and MNP. The dispersion slope will become steeper due to an increase in the inter-particle interaction distance R. If varying the value of the inter-particle distance R influences the process of quantum coherence and interference, therefore, the group velocity index can be controlled. The other factor can also affect the group velocity index, such as Rabi frequency Ω_c (see Fig. 7), and so on.

In the work, we apply an external coherent field and an external probe field, the SQD and the MNP are coupled via the Coulomb interaction. The total field felt by the SQD is changed owing to the existence of the MNP, and the internal field of the MNP to be involved. In the presence of MNP, the hybrid absorption vanishes, the transparency forms. Based on exciton/plasmonic induced transparency, the steep dispersion is formed in a relatively broad range around the plasmonic frequency. Thus, the group velocity index can be changed by adjusting the inter-particle interaction distance R between the SQD and MNP, the controllable group velocity of light is implemented from subluminal to superluminal.

Acknowledgement

This work is supported by the National Natural Science Foundation of China (Grant No. 211732 53) and China Post-doctoral Science Foundation (Grant No. 2011M5009 51).

References

[1] Zhang Wei, Govorov Alexander O, Bryant Garnett W. Phys Rev Lett 2006;97:146804.
[2] Artuso Ryan D, Bryant Garnett W. Nano Lett 2008;8:2106.
[3] Yan JY, Zhang W, Du SQ, Zhao XG, Govorov AO. Phys Rev B 2008;77:165301.
[4] Govorov Alexander O. Phys Rev B 2010;82:155322.
[5] Artuso Ryan D, Bryant Garnett W. Phys Rev B 2010;82:195419.
[6] Ridofo A, Di Stefano O, Fina N, Saija R, Savasta S. Phys Rev Lett 2010;105:263601.
[7] Artuso Ryan D, Bryant Garnett W. Phys Rev B 2011;83:235406.
[8] Sadeghi SM, Deng L, Li X, Huang W-P. Nanotechnology 2009;20:365401.
[9] Sadeghi SM. Nanotechnology 2009;20:225401.
[10] Xiao ZH, Zheng L, Lin HZ. Opt Expr 2012;20:1219.